Exposure to desflurane anesthesia confers colorectal cancer cells metastatic capacity through deregulation of miR-34a/LOXL3

Junyi Ren
Baoji University of Arts and Sciences
Xiaopeng Wang
Baoji central hospital
Gang Wei
Baoji central hospital
Yajing Meng (Yajing1Meng@hotmail.com)
Baoji University of Arts and Sciences https://orcid.org/0000-0002-8038-5507

Primary research

Keywords: desflurane, EMT, miR-34a, LOXL3

Posted Date: February 4th, 2020

DOI: https://doi.org/10.21203/rs.2.22615/v1

Version of Record: A version of this preprint was published on July 8th, 2020. See the published version at https://doi.org/10.1097/CEJ.0000000000000608.

Abstract

Background: Due to high potency and low toxicity, desflurane has been wildly used during surgery. Recent evidence that the use of desflurane was associated with colorectal cancer (CRC) tumor metastasis and poor prognosis raising concerns about the safety of desflurane. However, the mechanism was uncovered.

Methods: CRC cells were exposed to desflurane, the changes in morphology and epithelial-mesenchymal transition (EMT)-related genes were evaluated. Transwell assay was used to study the migration and invasion effect. Xenograft was performed to study the tumor formation ability of desflurane-treated cells in vivo. Dual luciferase reporter assay was conducted to verify the target of miR-34a. Knockdown or overexpression of LOXL3 was used to investigate the mechanism of desflurane-induced EMT. The association of LOXL3 with CRC molecular subtypes and clinical relevance was studied by analysis of public datasets.

Results: Exposure to desflurane induced EMT, migration, and invasion in CRC cells. Mice injected with desflurane-treated cells formed more tumors in the lungs. Downregulation of miR-34a and upregulation of LOXL3 were required for desflurane-induced EMT in CRC cells. LOXL3 was a direct target of miR-34a. Overexpression of LOXL3 rescued miR-34a-repressed EMT after exposure to desflurane. Elevated expression of LOXL3 was enriched in CMS4 and CRIS-B subtypes. Patients with high expression of LOXL3 showed more lymph node metastasis, as well as poor survival.

Conclusion: Desflurane induced EMT and metastasis in CRC through deregulation of miR-34a/LOXL3 axis. Clinical miR-34a mimic or inhibitor targeting LOXL3 might have a potential protective role when CRC patients anesthetized by desflurane.

Background

CRC is the third most common cancer but the second most common cause of cancer-related death [1]. Despite the big efforts in prevention, diagnosis, and treatment in the past decades, more than 1.8 million patients were diagnosed and 900, 000 individuals die in 2018 [2]. The leading cause of CRC death is metastasis. While surgery remains the most useful treatment for CRC, about 30% to 50% of patients suffered from cancer recurrence [3], which was considered due to the aggressive feature. However, recent reporters showed the surgery procedure, including anesthesia, could also accelerate the dissemination of cancer cells [4,5]. Iwasaki et al. studied the effect of three volatile anesthetics on human ovarian carcinoma and found all the anesthetics increased cell migration with 70 metastatic genes alteration[6]. Another study demonstrated that the use of desflurane for colon cancer surgery was associated with tumor metastasis and poor survival [7]. However, the mechanism underly desflurane associated metastasis in CRC has not been uncovered, although the desflurane has been wildly using[8,9].

Metastasis is a multi-step process, in which EMT is considered the first cascade that makes cancer cells spread from the primary site to other organs, such as liver and lung [10,11]. It has been shown that several

transcription factors (EF-TFs) including SNAIL and ZEB1 directly drive EMT in cancer cells [12]. During EMT, cancer cells in the primary site lose cell-cell adhesion and break through the basement membrane, later enter and exit the bloodstream through intravasation and extravasation, respectively [13]. subsequently, the cancer cell settles down and forms micrometastases [10,12]. Besides those EMT-TFs, other pro-tumor or anti-tumor genes regulates EMT by acting as upstream or downstream of the EMT-TFs. Among those anti-tumor genes, a well-known tumor-suppressor is miR-34a induced by p53 [14].

LOXL3 is one of the members of the LOX family composed of LOX, LOXL1, LOXL2, LOXL3, and LOXL4. Cellular LOXL3 is localized at the cytoplasm [15]. LOXL3 could interact with SNAIL, one of the most important EMT-TFs, thus repressed E-cadherin (CDH1) expression [16]. Moreover, LOXL3 was induced by TGF-β, which is an important signaling for EMT induction [17]. In a large cohort containing 597 primary gastric tumor cases, Kasashima et al. found that elevated expression of LOXL3 was positively correlated with tumor invasion, lymph node metastasis, and poor survival of patients [18].

Methods

Cell culture

DLD-1 and HT29 cell lines were obtained from the ATCC. Both cell lines were maintained in McCoy's 5A medium. The cells were propagated at 37 °C at 90% air humidity and with 5% CO_2.

Gas Exposure

Cells were placed in a special chamber with a volume of 2 L. the experimental gas was a mixture consisting of 21% oxygen, 5% carbon dioxide and 2% isoflurane, 3.6% sevoflurane or 10.3% desflurane. Nitrogen was used for balancing. The gas mixture was delivered to the gas chamber at a rate of 1.5 L/min until the expected concentration of desflurane was achieved. Subsequently, the chamber was placed in a cell culture incubation for a different duration. The concentration of desflurane in the chamber was monitored by an aesthetic analyzer.

RNA extraction, reverse transcription, and qPCR

Total RNA from cells from isolated with QIAGEN RNeasy Mini Kit (Cat No./ID: 74104) according to the manufacturer's instruction. cDNA was synthesized from 1 μg of total RNA each sample using anchored oligo(dT) primers (Verso cDNA Synthesis Kit, # AB1453B, Thermo Scientific). qPCR was performed by using the Fast SYBR Green Master Mix (Applied Biosystems). The primers for qPCR were listed in Supplementary Table 1.

Metastasis formation in NOD/SCID mice

$5*10^6$ DLD-1 cells with Luc2 gene were dissolved in 200 μl of sterile PBS and injected into 8-week old male immuno-compromised NOD/SCID mice through the tail vein. Anesthetized mice were injected

intraperitoneal with D-luciferin (150 mg/kg) and imaged 10 minutes after injection using the IVIS Illumina System (Caliper Life Sciences). The acquisition time was 1 minute. Mice were sacrificed and lungs were taken out, subsequently were stained with hematoxylin/eosin. The micro-metastasizes were counted.

Migration and invasion assays

Transwell bought from Corning was used to evaluate the ability of cell migration and invasion. For invasion assay, the inserts were coated with Matrigel. Cells were cultured in 6 well plates, the full culture medium was replaced with the serum-free medium one day before harvesting. Cells were harvested and the number was counted, subsequently, 100 ul of starved cells at a density of $5*10^6$/ml were added to the inserts, with 650 ul medium at the bottom served as an attractant. After 36 hours, the non-migrated or non-invasive cells were removed carefully and subjected to staining with 0.1% of crystal violet (diluted with PBS). The migrated or invasive cells were counted with microscopy.

Western blot

Cells were lysed with RIPA buffer (150 mM sodium chloride, 1.0% NP-40 or Triton X-100, 0.5% sodium deoxycholate, 0.1% sodium dodecyl sulfate, 50 mM Tris, pH 8.0) and subjected to sonication, followed by centrifugation at full speed at 4 ℃ for 20 min. BCA kit (#23225, Thermo Fisher Scientific) was used to measure the concentration of protein strictly according to the instruction. a total of 40 ug protein was loading in 7.5-12% SDS-PASE to separate, after which the protein was transferred to PVDF membrane. After blocked with 5% milk powder (diluted with TBST), the membrane was incubated with primary antibodies overnight. The next day, membranes were washed three times with TBST and subsequently incubated with secondary anti-mouse or anti-rabbit antibodies. The exposure was performed with the iBright CL1500 Imaging System (Thermo Fisher Scientific). Antibodies used for western blot were list in Supplementary Table 2.

Transfection

Cells were seeded in 6-well plates at a density of $1x10^6$ cells/ml one day before transfection. Cells were transfected with pcDNA or siRNA (siRNA LOXL3, #109785; siRNA control, # 4390843, Thermo Fisher Scientific) by using 15 µl Lipofectamine 2000 (Invitrogen) in 500 µl Opti-Mem I Medium (Gibco, Invitrogen-Life Technologies). After transfection, cells were incubated for 24 hours before refreshing the medium.

Cloning of wild type and mutated 3’-UTR of LOXL3

The 3'-UTR of human LOXL3 was amplified by PCR with the Verso cDNA kit (Thermo Scientific) and subsequently inserted to pGL3-control-MCS plasmid, which was further verified by sequencing. Mutation of the 3’-UTR of LOXL3 in the miR-34a binding site was generated by the QuikChange Mutagenesis Kit according to the manufacturer’s instructions (Stratagene).

Dual reporter assays

DLD-1 cells were seeded in 24-well plate at the density of $1*10^4$ cells/well one day before transfection. 20 ng of the indicated firefly luciferase reporter plasmid was transfected by Lipofectamine 2000 (Invitrogen), 5 ng of Renilla reporter plasmid used as a normalized control. In addition, 5 nM of miR-34a or a negative control oligonucleotide was transfected into DLD-1 cells. After incubation for 48 hours, the luciferase activity was measured by a Dual Luciferase Reporter assay kit (Promega) strictly according to the manufacturer's instruction.

Bioinformatic analysis

The RNA expression data from colorectal adenocarcinoma (COAD) patient samples was obtained from https://portal.gdc.cancer.gov/. pre-ranked Gene Set Enrichment Analysis (GSEA) was performed using the GSEA software (http://software.broadinstitute.org/gsea/index.jsp). Hallmark gene sets for GSEA were obtained from the Molecular Signatures Database (Broad Institute). GSE17536 and GSE37892 were obtained from the Gene Expression Omnibus (GEO) repository.

Statistical analysis

The Graph Prism version 8.0 software (https://www.graphpad.com/scientific-software/prism/) was used to generate statistical data. A Student´s t-test (unpaired, two-tailed) was used to determine significant differences between two groups of samples, while a 1-way analysis of variance followed by a Tukey multiple comparisons post-hoc test was performed for the comparison of multiple groups, A Pearson´s correlation was applied for correlation analyses. P-values < 0.05 were considered as significant (*: $p < 0.05$; **: $p < 0.01$; ***: $p < 0.001$).

Study approval

The animal protocols were approved by Baoji Central Hospital. All procedures involving human tumor biopsies were performed with the approval of the ethics committee of the Baoji Central Hospital.

Results

Desflurane induced EMT, migration, and invasion in CRC

To evaluate the potential effect of desflurane on CRC metastasis, the epithelial-like CRC cell line DLD-1 and HT29 were exposed to gas mixture constituting 21% oxygen, 5% carbon dioxide and 10.3% desflurane (an equal 1.7 minimum alveolar concentrations (MAC) in human of desflurane anesthetic concentrations) for 2 hours, followed by normal cell culture condition. After 48 hours, the morphology of both cell lines had changed to spindle-like, which is a typical characterization of EMT (Figure 1A). To further confirm and figure out whether this effect is time-dependent or independent, DLD-1 cells were exposed to desflurane for 0.5h, 2h, and 3h, respectively, and the EMT marker genes were quantified by qPCR. Mesenchymal markers *SNAIL*, *ZEB1*, and *VIM* were upregulated, while the epithelial marker *CDH1* (coding E-cadherin) was decreased (Figure 1B). Interestingly, these changes were not found when cells

exposed to desflurane for 0.5 hours. In addition, no significant difference in the EMT marker between the 2-hour-treated group and the 3-hour-treated group. Besides the mRNA level, the protein level of SNAIL, ZEB1 and VIM were increased, accompanied by a decrease of E-cadherin. Therefore, exposure to desflurane induced EMT in CRC cells in a time-independent manner (Figure 1C).

Since EMT initiates the spreading of tumor cells from the primary site to other organs via the bloodstream or lymphatic system, we asked whether desflurane affected the migration and invasion in CRC cells. Indeed, treatment with desflurane accelerated the closures in the scratch assay (Figure 1D). Moreover, transwell assay containing with or without matrigel showed that desflurane increased the ability of migration and invasion in DLD-1 cells (Figure 1E-F). To further confirm the EMT induction by desflurane, DLD-1 cells with or without treatment of desflurane were injected into mice through the tail vein. After 8 weeks, the mouse was sacrificed and the lung metastasis was analyzed by HE staining. Compared with the control group, the mouse injected with desflurane-treated formed more tumors in the lungs (Figure 1G-H). Therefore, desflurane-induced EMT was confirmed in vivo.

Downregulation of miR-34a was required for desflurane-induced EMT

Despite the EMT transcriptional factors such as SNAIL and ZEB1 which directly drive cells from epithelial to mesenchymal, miRNAs have been shown a critical role in the regulation of EMT or MET (mesenchymal-epithelial transition, a reverse biological process of EMT) [19,20]. To address whether miRNAs were involved in desflurane-induced EMT, we examined the expression changes of miRNAs after treatment with desflurane for 2 hours. According to literature, a panel of miRNAs with pro-metastasis or anti-metastasis ability were analyzed [21,22]. Among those miRNAs, miR-34a was the only one that dramatically decreased after treatment with desflurane, while other miRNAs showed no significant changes, suggesting that miR-34a was a potential mediator in desflurane-induced EMT (Figure 2A). As expected, restoration of miR-34a by a miR-34a mimic prevented the migration and invasion induced by desflurane (Figure 2B). Furthermore, the changes in EMT-markers induced by desflurane were also neutralized by the ectopic expression of miR-34a (Figure 2C-D). Antagomir mediated downregulation of miR-34a in a mesenchymal-like CRC cell line SW620, which has a higher level of endogenous miR-34a, reversed the changes in EMT markers altered by desflurane (Figure 2E). Moreover, antagomir miR-34a prevented the induction in cell invasion induced by desflurane (Figure 2F). Taken together, desflurane induced EMT through downregulation of miR-34a in CRC cells.

LOXL3 is a direct target of miR-34a

miR-34a is a tumor suppressor microRNA and exhibits anti-tumor function by repressing its downstream targets that contribute to cancer progression. To figure out which targets of miR-34a were involved in desflurane-induced EMT in CRC, we first analyzed the correlation between all the putative targets of miR-34a and EMT markers based on data from The Cancer Genome Atlas (TCGA). According to the correlation, several genes were picked up and further analyzed. Before experimental validation of the putative targets of miR-34a, we checked the effects of those genes in desflurane-induced cell migration

and invasion by using siRNAs. siRNA-mediated downregulation of LOXL3 dramatically prevented the increased migration and invasion capacity of DLD-1 cells induced by desflurane (data not shown). Therefore, we focused on LOXL3.

The seed-matching sequence in 3'-UTR of *LOXL3* for miR-34a is conserved in human, mouse and other species, implying the evolutional importance of miR-34a/ LOXL3 axis (Figure 3A). Analysis of the TCGA database, which contains 461 primary CRC samples, showed mRNA expression of *LOXL3* was inversely correlated with miR-34a (Figure 3B). In addition, ectopic expression of miR-34a mimics resulted in the downregulation of LOXL3 at both mRNA and protein levels (Figure 3C-E). Furthermore, reporter constructs containing the 3'-UTR of *LOXL3* including the seed-matching sequence were repressed by co-transfection of miR-34a mimic, but not when the seed-matching sequence was mutated, demonstrating that LOXL3 was a direct target of miR-34a (Figure 3F).

LOXOL3 induced EMT, migration, and invasion in CRC cells

Gene Sets Enrichment Analysis (GSEA) showed *LOXL3* expression from TCGA was highly enriched in the EMT gene signature, which was further validated by another two cohorts (Figure 4A). In further, *LOXL3* was positively associated with EMT-TFs, while negatively associated with epithelial related genes, such as *CDH1* and *TJP1* (also known as *ZO-1*; Figure 4B). Ectopic expression of LOXL3 in DLD-1 cells induced SNAIL, ZEB1, VIM, and repressed E-cadherin (Figure 4C). Moreover, overexpression of LOXL3 increased cell capacity of migration and invasion (Figure 4D). siRNA-mediated knockdown of LOX3 in a mesenchymal-like cell line SW480 (with high expression of SNAIL/ZEB1/VIM, and high migration and invasion capacity) downregulated EMT marker genes and inhibited cell migration and invasion (Figure 4E). Therefore, LOXL3 itself has the ability to induce EMT, migration, and invasion in CRC.

Deregulation of miR-34/LOXL3 axis contribute to desflurane-induced EMT

Next, we addressed whether miRNA-34a/LOXL3 was involved in desflurane-induced EMT. As expected, LOXL3 was upregulated after desflurane treatment, while it was repressed by ectopic expression of miR-34a (Figure 5A). Furthermore, the siRNA-mediated knockdown of LOXL3 protected cells from desflurane-induced EMT, migration, and invasion (Figure 5B-C). Overexpression of LOXL3 lacking miR-34a binding site rescued the decrease of EMT, migration, and invasion induced by ectopic miR-34a expression after exposure to desflurane (Figure 5D-E). Taken together, the disorder of the miR-34a/LOXL3 axis contributed to the EMT, migration, and invasion induced by exposure of desflurane.

The clinical relevance of LOXO3

Since EMT is required for cancer metastasis which is the leading cause of cancer-related death, we wondered whether miR-34a/LOXL3 axis was clinical relevance. As miR-34a is a powerful tumor suppressor in CRC and had been well studied previously [23-25], here we investigated the role of LOXL3 in CRC clinical outcomes and features. Recently, the molecular subtypes of CRC base on gene expression have been proposed, which correlate gene expression with tumor behavior. Consensus molecular

subtypes (CMS) of CRC represents one of the robust subtypes classifications and have been wildly accepted. Therefore, we first performed an analysis of the correlation between *LOXL3* and molecular subtypes in CRC. Analysis of primary tumors from TCGA and another two datasets showed higher expression of *LOXL3* were enriched in the CMS4 subtype (Figure 6A), which was characterized by EMT gene signature and poor survival. Since the CMS classification is base-on gene expression of primary tumor samples, the samples might be contaminated by stromal cells. Besides the patients with higher expression of LOXL3 in the whole tumors have poor survival, we also wanted to figure out that the features of tumor cells with a higher level of *LOXL3*. Therefore, we used another molecular subtype classification which bases on patient's derived xenografts (PDX), and the contaminated mRNA from mouse stromal cells had been filtered, thus the classification was based on cancer cell-intrinsic gene expression. Among the five CRC intrinsic subtypes (CRISA-B), *LOX3L* was enriched in the CRIS-B subtype, which was also characterized by EMT and poor prognosis (Figure 6B).

As both CMS and CRIS classification showed LOXL3 was strongly associated with EMT and poor survival, we next analyzed the association of *LOXL3* with CRC patients' survival. Analysis of the TCGA database showed patients with a higher mRNA level of *LOXL3* had poor survival (Figure 6C). Furthermore, increased expression of *LOXL3* was associated with CRC patients' lymph node metastasis (Figure 6D), and the expression level of LOXL3 was positively associated with the degree of lymph node metastasis (Figure 6E).

Discussion

The FDA-approved indications for desflurane are induction or maintenance of anesthesia in adults [8]. In recent years, desflurane has been wildly used in surgical procedures and replaced other general anesthetics such as isoflurane and sevoflurane to be the first choice due to its apparent advances including strong potency and low toxicity [7,26]. Evidence that the use of desflurane in surgery for CRC was associated with tumor metastasis and poor prognosis raising concerns in clinical use [6,7]. Here, we showed that exposure of CRC cells to desflurane induced EMT, migration, and invasion, as evidenced by changes in morphology and EMT markers. Interestingly, exposure to desflurane a short time had no effect on DLD-1 cells. Furthermore, xenograft confirmed that the induction of EMT by desflurane is true in vivo.

miRNA is a small non-coding RNA molecule (containing about 21-25 nucleotides) found in plants, animals and some viruses [27]. It regulates gene expression by target gene with the seed-matching sequence, results in the degradation of target genes [27,28]. It has been estimated that more than 60% of human protein-coding genes are regulated by miRNAs [28]. Each miRNA has hundreds of potential target genes, leading to complicated and contradictory effects [29]. miR-34a is a member of miR-34 family and was first identified as a downstream of the tumor suppressor gene p53 [30]. Since the relationship with p53, it has attracted a lot of investigators to focus on its anti-tumor function [19,20,23,24,31]. So far, it has been clear that miR-34a exhibits tumor-suppressive function in CRC by targeting multiple genes, such as IL6, MYC, CD44, and c-Kit [32-35]. Many types of cancer initiation and progression were accompanied by the

downregulation of miR-34a [36,37]. Here, the downregulation of miR-34a was found again when treatment with desflurane, suggesting that a clinical miR-34a mimic might have a potential protective role in antagonizing the effect of desflurane during surgery for CRC.

Despite miR-34a, the induction of EMT by desflurane was accompanied by the upregulation of SNAIL and LOXL3. The previous study showed LOXL3 physically interacts and cooperates with SNAIL to downregulate E-cadherin expression, which is a critical marker for epithelial cells [16]. Since SNAIL represses the expression of miR-34a by directly binding to its promoter [38], it is presumed that the downregulation of miR-34a was further strengthened by the interaction of LOXL3 and SNAIL. As a consequence of this positive feedback loop, the desflurane-induced EMT was further enhanced.

Conclusion

LOXL3 represents a novel potential target for CRC treatment. A clinical miR-34a mimic or inhibitor targeting LOXL3 might have a potential protective role when CRC patients anesthetized by desflurane.

Abbreviations

CDH1: E-Cadherin

CMS: Consensus Molecular Subtype

COAD: Colon Adenocarcinoma

CRC: Colorectal Cancer

CRIS: Colorectal Cancer Intrinsic Subtypes

EMT：Epithelial-Mesenchymal Transition

MET: Mesenchymal-Epithelial Transition

EMT-TF：EMT-inducing transcription factor

GSEA: Gene Set Enrichment Analyses

TCGA: The Cancer Genome Atlas

3'-UTR: Three Prime Untranslated Region

miRNAs: microRNAs

Declarations

Ethics approval and consent to participate：

The animal protocols were approved by Baoji Central Hospital. All procedures involving human tumor biopsies were performed with the approval of the ethics committee of the Baoji Central Hospital.

Consent for publication

All the authors agree to the publication clause.

Availability of data and material

The datasets generated and/or analyzed during the current study are available from the corresponding author on reasonable request.

Competing interests

The authors declare that they have no competing interests.

Funding

This study was funded by Baoji Maternal and Child Health Hospital

Author Contributions:

JR: Designed and performed experiments, analyzed results, wrote the paper; XW: bioinformatics analysis and initial experiments; GW: xenograft analysis; YM: conceived and supervised the study, planned experiments and wrote the paper.

References

1. Siegel RL, Miller KD, Fedewa SA, et al. Colorectal cancer statistics, 2017. *CA Cancer J Clin.* 2017;67(3):177-193.
2. Keum N, Giovannucci E. Global burden of colorectal cancer: emerging trends, risk factors and prevention strategies. *Nat Rev Gastroenterol Hepatol.* 2019;16(12):713-732.
3. Zare-Bandamiri M, Fararouei M, Zohourinia S, Daneshi N, Dianatinasab M. Risk Factors Predicting Colorectal Cancer Recurrence Following Initial Treatment: A 5-year Cohort Study. *Asian Pac J Cancer Prev.* 2017;18(9):2465-2470.
4. Yang W, Cai J, Zabkiewicz C, Zhang H, Ruge F, Jiang WG. The Effects of Anesthetics on Recurrence and Metastasis of Cancer, and Clinical Implications. *World J Oncol.* 2017;8(3):63-70.
5. Deng F, Ouyang M, Wang X, et al. Differential role of intravenous anesthetics in colorectal cancer progression: implications for clinical application. *Oncotarget.* 2016;7(47):77087-77095.
6. Iwasaki M, Zhao H, Jaffer T, et al. Volatile anaesthetics enhance the metastasis related cellular signalling including CXCR2 of ovarian cancer cells. *Oncotarget.* 2016;7(18):26042-26056.

7. Wu ZF, Lee MS, Wong CS, et al. Propofol-based Total Intravenous Anesthesia Is Associated with Better Survival Than Desflurane Anesthesia in Colon Cancer Surgery. *Anesthesiology.* 2018;129(5):932-941.
8. Landoni G, Lomivorotov VV, Nigro Neto C, et al. Volatile Anesthetics versus Total Intravenous Anesthesia for Cardiac Surgery. *N Engl J Med.* 2019;380(13):1214-1225.
9. Nury H, Van Renterghem C, Weng Y, et al. X-ray structures of general anaesthetics bound to a pentameric ligand-gated ion channel. *Nature.* 2011;469(7330):428-431.
10. Nieto MA, Huang RY, Jackson RA, Thiery JP. Emt: 2016. *Cell.* 2016;166(1):21-45.
11. Jackstadt R, van Hooff SR, Leach JD, et al. Epithelial NOTCH Signaling Rewires the Tumor Microenvironment of Colorectal Cancer to Drive Poor-Prognosis Subtypes and Metastasis. *Cancer Cell.* 2019;36(3):319-336 e317.
12. Lamouille S, Xu J, Derynck R. Molecular mechanisms of epithelial-mesenchymal transition. *Nat Rev Mol Cell Biol.* 2014;15(3):178-196.
13. Tsai JH, Yang J. Epithelial-mesenchymal plasticity in carcinoma metastasis. *Genes Dev.* 2013;27(20):2192-2206.
14. He L, He X, Lowe SW, Hannon GJ. microRNAs join the p53 network–another piece in the tumour-suppression puzzle. *Nat Rev Cancer.* 2007;7(11):819-822.
15. Ma L, Huang C, Wang XJ, et al. Lysyl Oxidase 3 Is a Dual-Specificity Enzyme Involved in STAT3 Deacetylation and Deacetylimination Modulation. *Mol Cell.* 2017;65(2):296-309.
16. Peinado H, Del Carmen Iglesias-de la Cruz M, Olmeda D, et al. A molecular role for lysyl oxidase-like 2 enzyme in snail regulation and tumor progression. *EMBO J.* 2005;24(19):3446-3458.
17. Sethi A, Mao W, Wordinger RJ, Clark AF. Transforming growth factor-beta induces extracellular matrix protein cross-linking lysyl oxidase (LOX) genes in human trabecular meshwork cells. *Investigative ophthalmology & visual science.* 2011;52(8):5240-5250.
18. Kasashima H, Yashiro M, Okuno T, et al. Significance of the Lysyl Oxidase Members Lysyl Oxidase Like 1, 3, and 4 in Gastric Cancer. *Digestion.* 2018;98(4):238-248.
19. Rokavec M, Li H, Jiang L, Hermeking H. The p53/miR-34 axis in development and disease. *J Mol Cell Biol.* 2014;6(3):214-230.
20. Rokavec M, Li H, Jiang L, Hermeking H. The p53/microRNA connection in gastrointestinal cancer. *Clin Exp Gastroenterol.* 2014;7:395-413.
21. Chan SH, Wang LH. Regulation of cancer metastasis by microRNAs. *J Biomed Sci.* 2015;22:9.
22. Kim J, Yao F, Xiao Z, Sun Y, Ma L. MicroRNAs and metastasis: small RNAs play big roles. *Cancer Metastasis Rev.* 2018;37(1):5-15.
23. Oner MG, Rokavec M, Kaller M, et al. Combined Inactivation of TP53 and MIR34A Promotes Colorectal Cancer Development and Progression in Mice via Increasing Levels of IL6R and PAI1. *Gastroenterology.* 2018.

24. Li H, Rokavec M, Jiang L, Horst D, Hermeking H. Antagonistic Effects of p53 and HIF1A on microRNA-34a Regulation of PPP1R11 and STAT3 and Hypoxia-induced Epithelial to Mesenchymal Transition in Colorectal Cancer Cells. *Gastroenterology.* 2017;153(2):505-520.
25. Jiang L, Hermeking H. miR-34a and miR-34b/c Suppress Intestinal Tumorigenesis. *Cancer research.* 2017;77(10):2746-2758.
26. Kapoor MC, Vakamudi M. Desflurane - revisited. *J Anaesthesiol Clin Pharmacol.* 2012;28(1):92-100.
27. Ganser LR, Kelly ML, Herschlag D, Al-Hashimi HM. The roles of structural dynamics in the cellular functions of RNAs. *Nat Rev Mol Cell Biol.* 2019;20(8):474-489.
28. Gebert LFR, MacRae IJ. Regulation of microRNA function in animals. *Nat Rev Mol Cell Biol.* 2019;20(1):21-37.
29. Bracken CP, Scott HS, Goodall GJ. A network-biology perspective of microRNA function and dysfunction in cancer. *Nat Rev Genet.* 2016;17(12):719-732.
30. Hermeking H. p53 enters the microRNA world. *Cancer Cell.* 2007;12(5):414-418.
31. Hunten S, Kaller M, Drepper F, et al. p53-Regulated Networks of Protein, mRNA, miRNA, and lncRNA Expression Revealed by Integrated Pulsed Stable Isotope Labeling With Amino Acids in Cell Culture (pSILAC) and Next Generation Sequencing (NGS) Analyses. *Mol Cell Proteomics.* 2015;14(10):2609-2629.
32. Rokavec M, Oner MG, Li H, et al. IL-6R/STAT3/miR-34a feedback loop promotes EMT-mediated colorectal cancer invasion and metastasis. *J Clin Invest.* 2014;124(4):1853-1867.
33. Yamamura S, Saini S, Majid S, et al. MicroRNA-34a modulates c-Myc transcriptional complexes to suppress malignancy in human prostate cancer cells. *PloS one.* 2012;7(1):e29722.
34. Liu C, Kelnar K, Liu B, et al. The microRNA miR-34a inhibits prostate cancer stem cells and metastasis by directly repressing CD44. *Nat Med.* 2011;17(2):211-215.
35. Siemens H, Jackstadt R, Kaller M, Hermeking H. Repression of c-Kit by p53 is mediated by miR-34 and is associated with reduced chemoresistance, migration and stemness. *Oncotarget.* 2013;4(9):1399-1415.
36. Hermeking H. MiR-34a and p53. *Cell cycle.* 2009;8(9):1308.
37. He L, He X, Lim LP, et al. A microRNA component of the p53 tumour suppressor network. *Nature.* 2007;447(7148):1130-1134.
38. Hahn S, Jackstadt R, Siemens H, Hunten S, Hermeking H. SNAIL and miR-34a feed-forward regulation of ZNF281/ZBP99 promotes epithelial-mesenchymal transition. *EMBO J.* 2013;32(23):3079-3095.

Tables

Table 1 qPCR primers

gene	forward (5′-3′)	reverse (5′-3′)
β-actin	TGACATTAAGGAGAAGCTGTGCTAC	GAGTTGAAGGTAGTTTCGTGGATG
VIM	TACAGGAAGCTGCTGGAAGG	ACCAGAGGGAGTGAATCCAG
CDH1	CCCGGGACAACGTTTATTAC	GCTGGCTCAAGTCAAAGTCC
pri-miR-34a	CGTCACCTCTTAGGCTTGGA	CATTGGTGTCGTTGTGCT
SNAIL	GCACATCCGAAGCCACAC	GGAGAAGGTCCGAGCACAC
ZEB1	TCAAAAGGAAGTCAATGGACAA	GTGCAGGAGGGACCTCTTTA

Table 2 antibodies

epitope	species	catalog no.	company	dilution	source
Vimentin	human	#5741	Cell Signaling	1:1000	rabbit
ZEB1	human	3396	Cell Signaling	1:1000	rabbit
E-cadherin	human	#14472	Cell Signaling	1:1000	mouse
α-tubulin	human	#3873	Cell Signaling	1:1000	mouse
SNAIL	human	# 3879	Cell Signaling	1:1000	rabbit

Figures

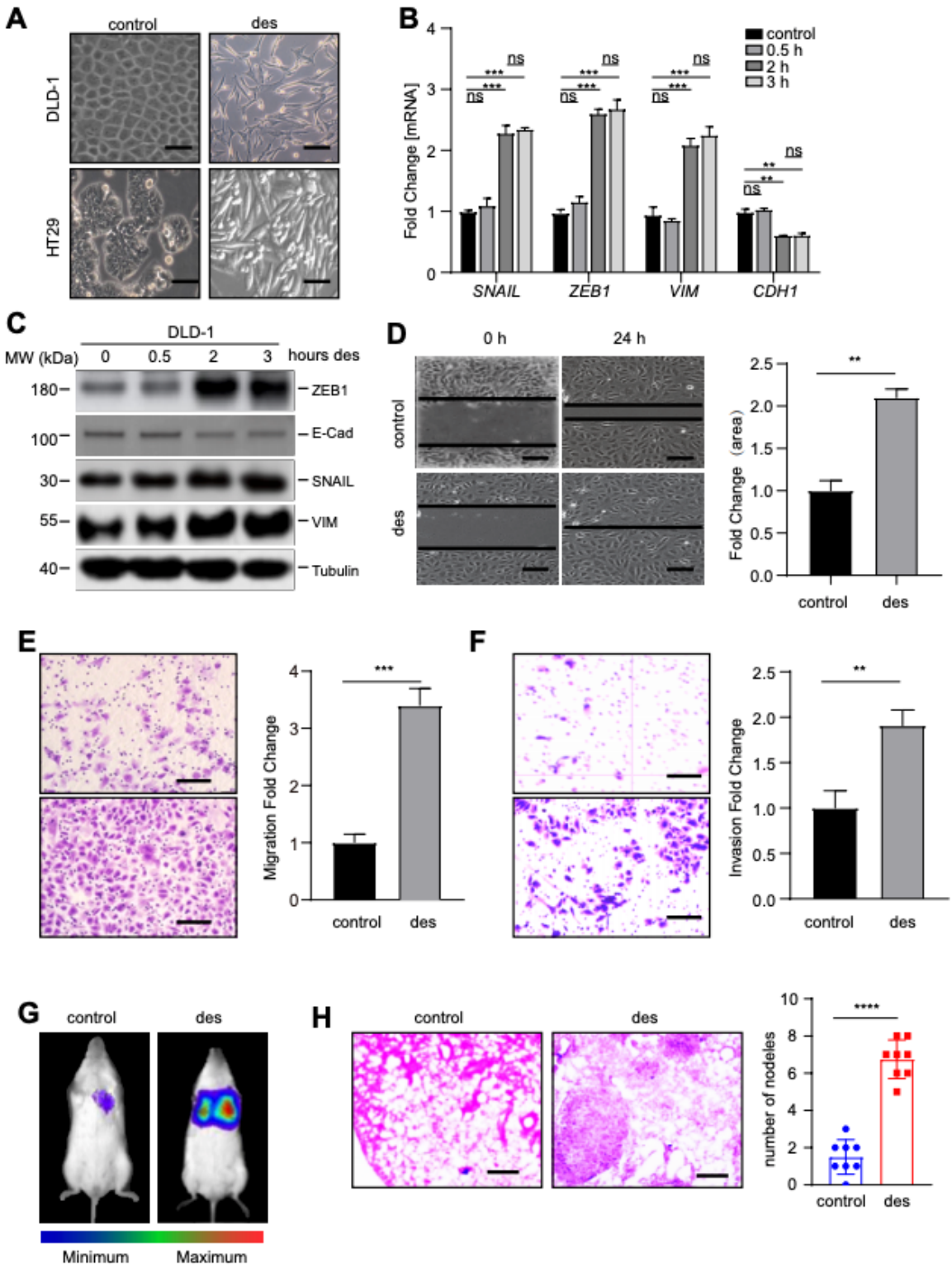

Figure 1

Exposure to desflurane induced EMT, migration, and invasion in CRC cells. A, DLD-1 and HT29 cells were exposed to desflurane for 3 hours, followed by normal incubation conditions for 48 hours. And the morphology was captured by a phase-contrast microscope. Scale bar: 100 μm B, C, qPCR (B) and western analysis (C) of indicated mRNA or proteins after DLD-1 cells were exposed to desflurane for 0.5, 2, 3 hours respectively. D, Scratch assay of DLD-1 cells. After 24 hours, the area of “wound” was measured

and analyzed. Scale bar: 100 µm E, F, transwell with or without Matrigel were used to study the migration (E) and invasion (F) capacity of DLD-1 cells after treatment with desflurane for 2 hours. Scale bar: 100 µm G, Representative examples of bioluminescence imaging 8 weeks after the injection of pre-treated DLD-1 cells in. H, Representative pictures of H&E staining of lung metastasis (left). the number of micro-metastasizes was counted (right). Scale bar: 500 µm In B, D, E, F, and H mean values ± SD (n = 3) are provided. *P < 0.05; **P < 0.01; *** P < 0.001; **** P < 0.0001.

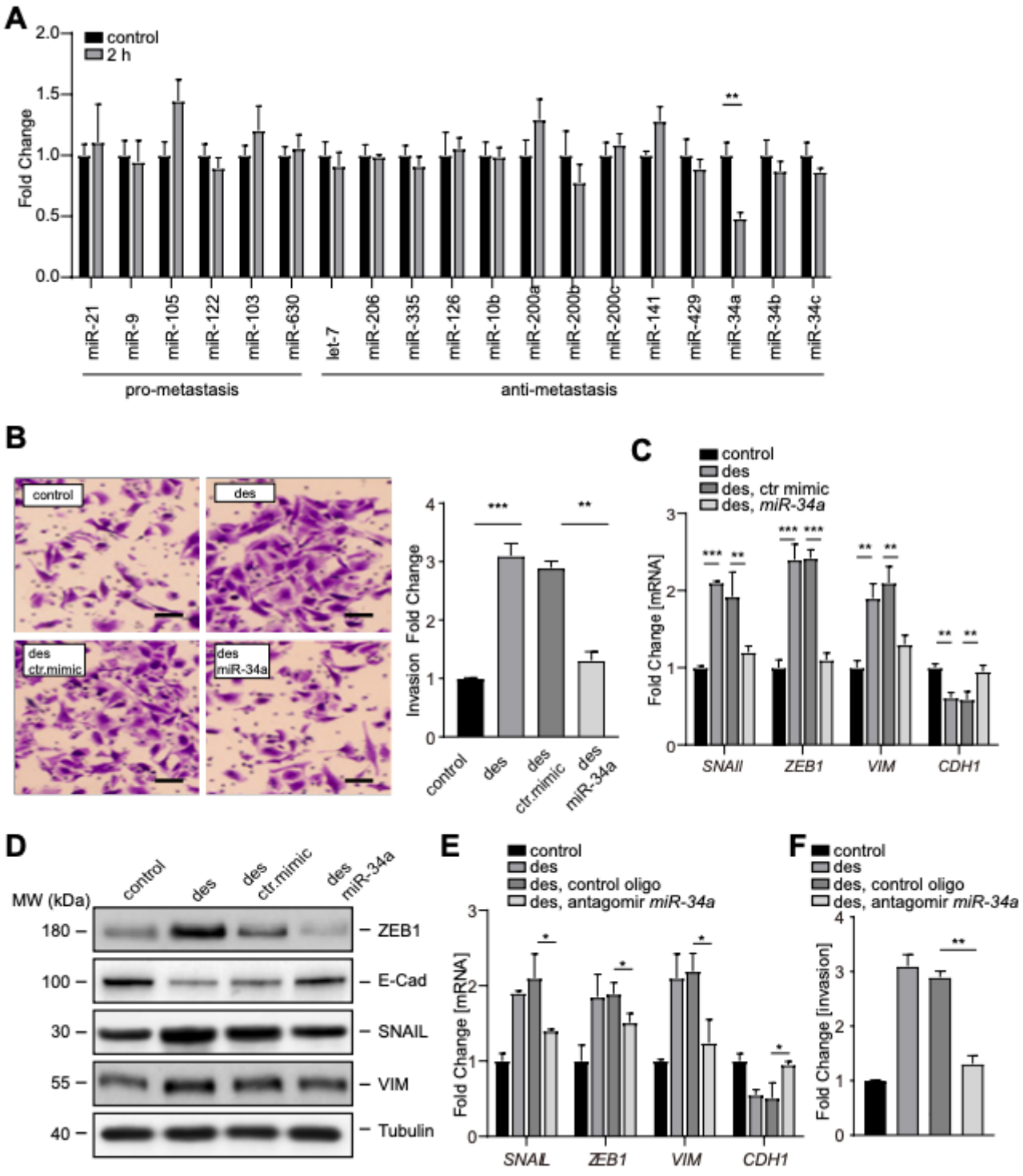

Figure 2

Downregulation of miR-34a was required for desflurane-induced EMT A, a panel of miRNAs was measured after DLD-1 cells exposed to desflurane for 2 hours. B, DLD-1 cells exposed to desflurane for 2 hours, and subsequently were transfected with miR-34a mimic, followed by 48 hours incubation. Cells were subjected to transwell with Matrigel. Scale bar: 100 μm C, D, Cells were treated as described above, the indicated mRNA (C) or proteins (D) were analyzed by qPCR or western blot, respectively. E, after DLD-1 cell exposed to desflurane for 2 hours, antagomir miR-34a were transfected with lipofectamine 2000, followed by 48 hours incubation. Subsequently, cells were harvested and subjected to qPCR analysis. F, DLD-1 cells were treated as same as figure 2E. Transwell assay was performed to study the capacity of invasion. In A, B, C, E, and F mean values ± SD (n = 3) are provided. *P < 0.05; **P < 0.01; *** P < 0.001.

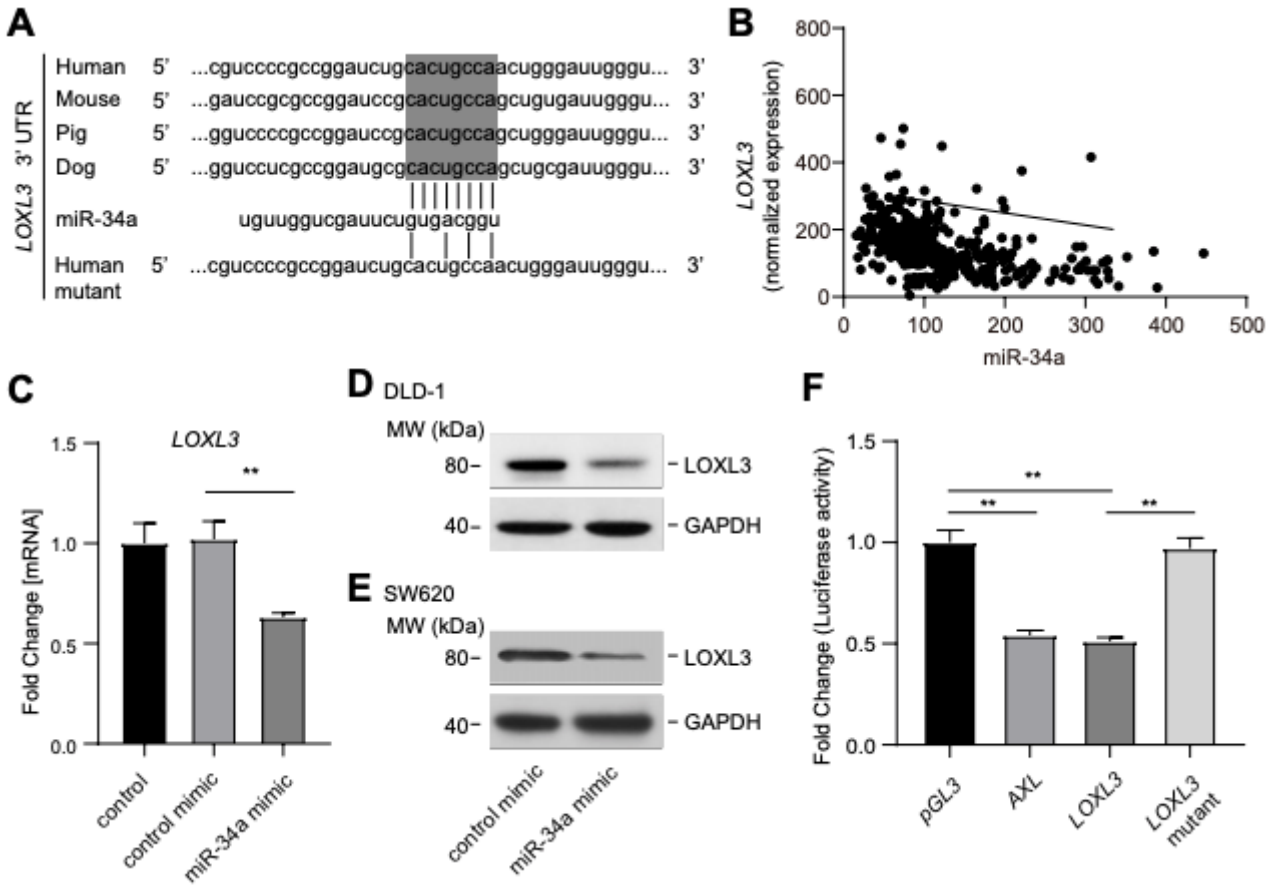

Figure 3

LOXL3 is a direct target of miR-34a A, Schematic representation of the LOXL3 wild type or mutated 3'-UTR indicating seed-matching sequences and miR-34 seed sequences. The black vertical bars indicate possible base pairing. B, The correlation of LOXL3 mRNA and mature miR-34a from the TCGA database. C, DLD-1 cells were transfected with control mimic or miR-34a mimic, the mRNA of LOXL3 were analyzed by qPCR. D, E, DLD-1 or HT29 cells were transfected with control mimic or miR-34a mimic, the protein of LOXL3 was measured by western blot. F, Dual luciferase reporter assay in DLD-1 cells 48 h after transfection with control mimic or miR-34a mimic and the empty pGL3 vector or pGL3 harboring the indicated 3'-UTR-reporter constructs. A 3'-UTR reporter of the known miR-34a target AXL served as a positive control. In C and F mean values ± SD (n = 3) are provided. *P < 0.05; **P < 0.01; *** P < 0.001.

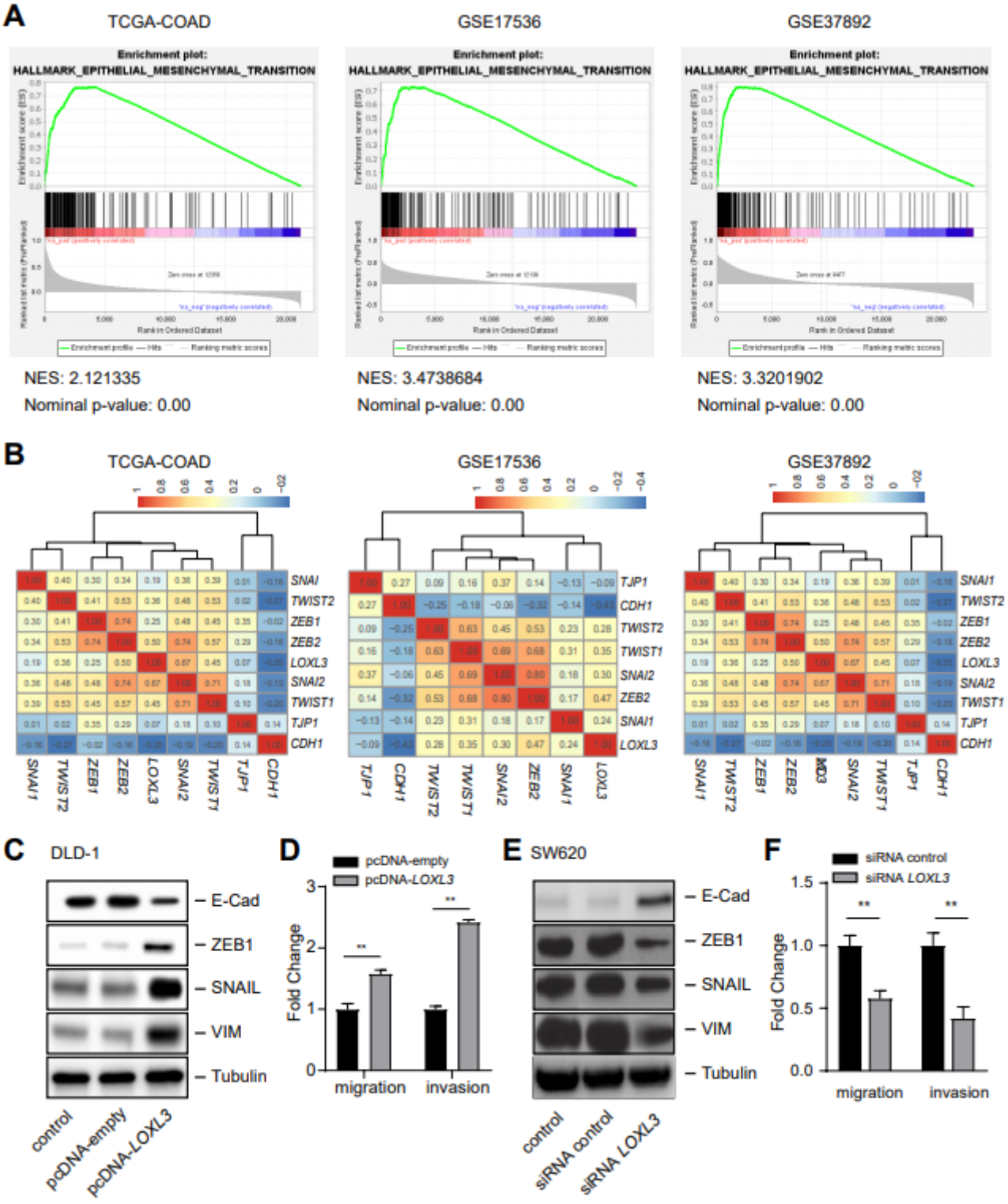

Figure 4

LOXL3 induced EMT, migration, and invasion A, mRNA of LOXL3 from TCGA, GSE17536, and GSE37892 were pre-ranked according to the correlation coefficient with the other genes, and subsequently performed the Gene Set Enrichment Analysis (GSEA). B, Heatmap showing the correlation coefficient between LOXL3 and known EMT transcription factors. C, Western blot analysis of indicated proteins after DLD-1 cells were transfected with indicated vectors for 72 hours. D, After DLD-1 cells were transfected with indicated

vectors for 24 hours, cells were subjected to transwell with or without Matrigel to study the capacity of migration and invasion. E, Western blot analysis of indicated proteins after SW620 cells were transfected with siRNA control or siRNA LOXL3 for 72 hours. F, After SW620 cells were transfected with siRNA control or siRNA LOXL3 for 24 hours, cells were subjected to transwell with or without Matrigel to study the capacity of migration and invasion. In D and F mean values ± SD (n = 3) are provided. *P < 0.05; **P < 0.01; *** P < 0.001.

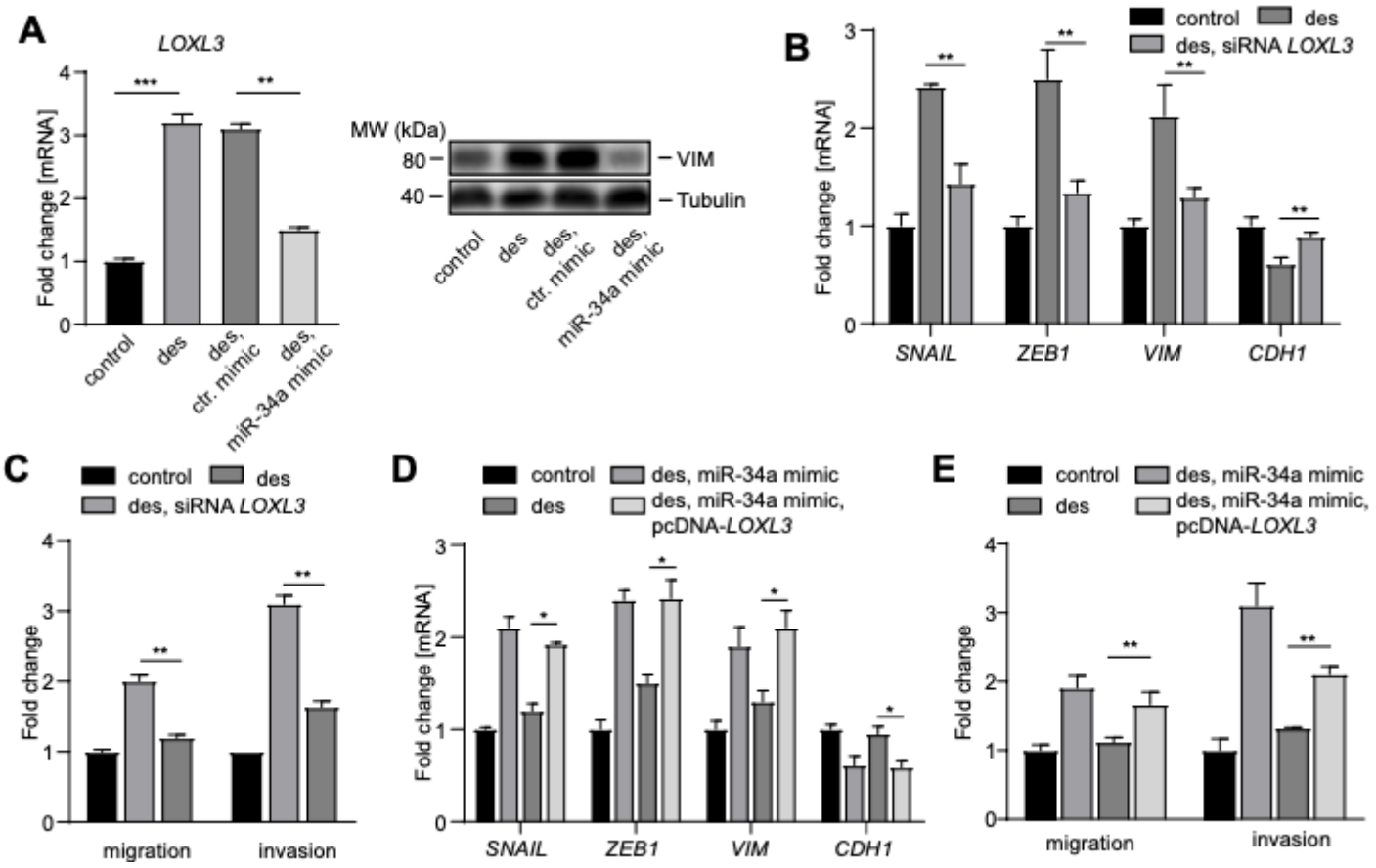

Figure 5

Deregulation of miR-34a/LOXL3 was involved in desflurane-induced EMT A, After DLD-1 cells were treated with or without desflurane 2 hours, cells were transfected with or without control mimic or miR-34a mimic, followed by incubated for 48 hours or 72 hours, cells were harvested and subjected to qPCR and western analysis. B, DLD-1 cells were transfected with siRNA LOXL3 after exposure to desflurane, the indicated mRNA were analyzed by qPCR. C, DLD-1 cells were treated with desflurane for 2 hours and subsequently transfected with siRNA LOXL3 for 24 hours. Then the cells were subjected to migration and invasion assay. D, E, Cells were transfected with miR-34 mimic after exposure to desflurane, 12 hours after transfection, pcDNA-LOXL3 lacking miR-34a binding site in the 3'-UTR was transfected into cells. Subsequently, cells were subjected to qPCR (D) and transwell assay (E), respectively. In A, B ,C, D and E mean values ± SD (n = 3) are provided. *P < 0.05; **P < 0.01.

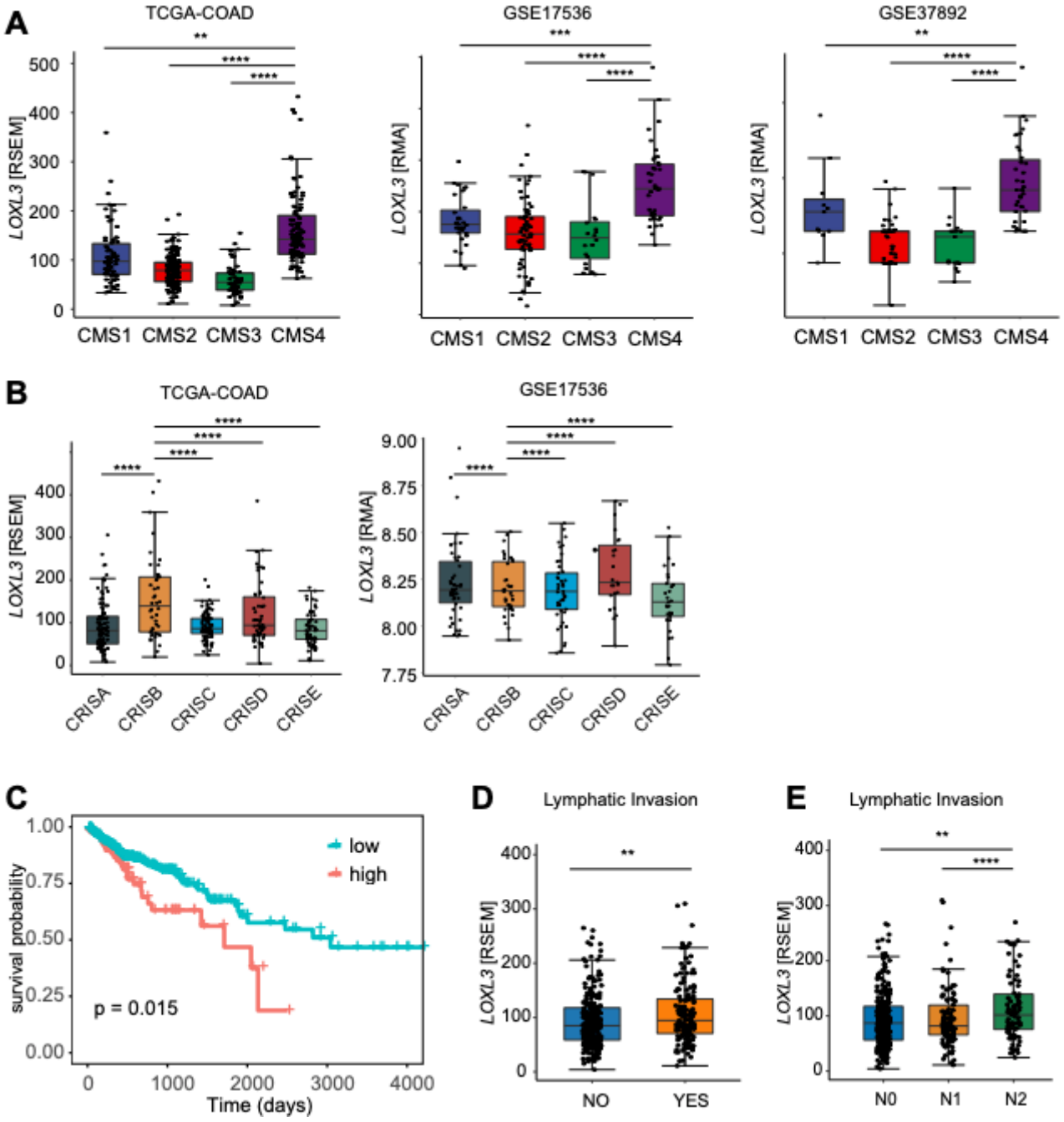

Figure 6

The clinical relevance of LOXL3 A, B, Analysis of LOXL3 mRNA from TCGA, GSE17536, and GSE 37892 belonging to the indicated consensus molecular subtypes (CMS) or CRC intrinsic subtypes (CRIS). C, Association of LOXL3 mRNA expression with overall survival in the TCGA COAD dataset. D, E, Association of LOXL3 mRNA expression with the status of lymph node metastasis. In A, B, D and E mean values ± SD (n = 3) are provided. *P < 0.05; **P < 0.01; *** P < 0.001; **** P < 0.0001.